

# PF1/PF2: A Molecular Mechanics Force Field for Conformational Studies on Oxygen and Sulphur Compounds

## PF1/PF2: Um Campo de Forças Mecânico-Molecular para o Estudo Conformacional de Compostos de Oxigénio e Enxofre

RUI FAUSTO

DEPARTAMENTO DE QUÍMICA, UNIVERSIDADE DE COIMBRA, P - 3049 COIMBRA (PORTUGAL)

Potential energy functions and important details of computational procedures currently used in Molecular Mechanics are reviewed. The general orientation followed during the development of the PF1/PF2 force fields and a series of selected results are also presented and analysed to illustrate the efficiency and reliability of these force fields, as applied to conformational and vibrational studies on oxygen and sulphur compounds.

Neste artigo, são discutidas as funções de energia potencial e os aspectos mais relevantes dos procedimentos computacionais correntemente utilizados em Mecânica-Molecular. Apresenta-se a orientação geral seguida durante o desenvolvimento do campo de forças PF1/PF2, e discute-se uma série seleccionada de resultados com ele obtidos, tendo em vista ilustrar a eficácia e poder predictivo quando aplicado ao estudo conformacional e vibracional de compostos de oxigénio ou enxofre.

### Introduction

In contrast to the more sophisticated quantum mechanical treatments, the conventional and intuitive description of a molecule with specific bonds between atoms has attracted the growing preference of many scientists for methods, like Molecular Mechanics (MM), that implement a classical representation of molecules and compete with Quantum Mechanics in the quality of the results.

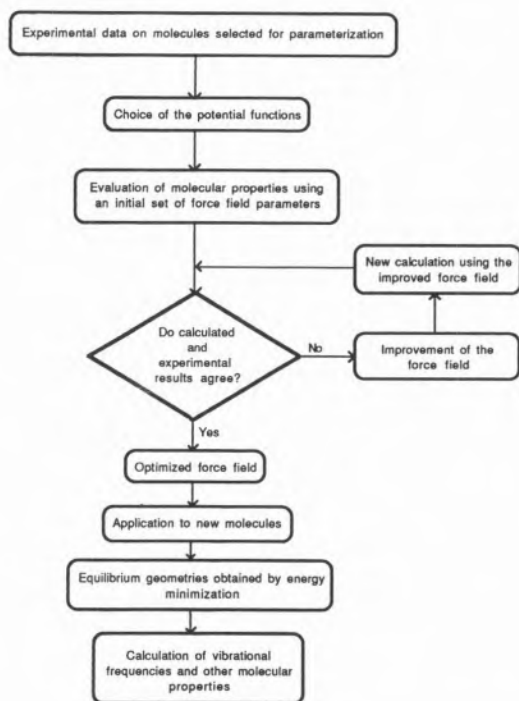
The general principles of MM were laid down fifty years ago [1]. In some small and simple molecules, it was assumed that the molecular geometry would adjust itself to the "natural" values of bond lengths and bond angles. In more complex systems, van der Waals interactions between non-bonded atoms and correlations between bond angles could cause deviations from those values. Comparison between the geometries of the real and model systems was used to measure the strain within the molecule and evaluate specific molecular properties, like geometries, vibrational frequencies and thermodynamic properties.

A complete molecular mechanical calculation involves four fundamental steps:

- i) the choice of potential energy functions that correspond to different types of interactions;
- ii) the force field parameterization;
- iii) the calculation of molecular equilibrium geometries through energy minimization;
- iv) the calculation of other molecular properties considering the previously determined equilibrium geometries.

The possibility of calculating a large number of properties is one of the most relevant features of MM. However, its most fundamental characteristic is related with the empirical consistency of the method, imparting a high degree of confidence to the results [2]. In fact, properties of a given molecule are calculated using a set of potential energy parameters previously developed to reproduce experimental values in simpler molecules of the same family.

While the properties considered in a MM study display a large variety and a diverse nature, a general agreement between calculated and experimental values is reached, provided a judicious choice of both potential energy functions and model compounds is performed.



Since MM offers an attractive means of undertaking conformational and vibrational analysis, we have begun to develop this technique in our laboratory with a view to applying it to the most important families of oxygen and sulphur containing molecules. As a starting point, we have developed a MM force field for simple acyl chlorides, carboxylic acids and esters which can also be used to deal with alkanes, alcohols and ethers (**PF1**) [3,4]. This force field was later applied to  $\alpha$ -chloro substituted carbonyl compounds, mainly to assess conformational freedom involving rotation around the  $C_\alpha-C(=O)$  bond [5-7] and, more recently, extended to deal with both the aldehyde and ketone functional groups [8]. The general quality of the results obtained with the **PF1** force field for these families of oxygen containing molecules has been discussed in detail [9,10] and improves on previously reported MM calculations despite its simplicity.

The extension of **PF1** force field to sulphur containing molecules, named **PF2**, has been successfully carried out more recently and proved to be of great value in studying this kind of molecules [10-12]. Being the first MM force field that can be applied to thiocarbonyl compounds, **PF2** can be used to deal with thiols, thioethers, thioaldehydes, thiones, dithioacids and dithioesters, thus covering a large series of different functional groups.

In this paper, we discuss the general orientation that has been followed during the development of the **PF1/PF2** force fields, with particular emphasis on the selection of potential energy functions. A series of results are also presented and analysed to illustrate the

efficiency and reliability of these force fields, as applied to oxygen and sulphur compounds.

## Potential functions

Molecular Mechanics assumes the potential energy as a sum of terms depending on the molecular geometry:

$$E = E_v + E_\delta + E_t + E_{nb} + \dots \quad (1)$$

$E$ , sometimes named "steric energy" [1,2], represents the difference between the energies of the real molecule and the hypothetical molecule where all the structural parameters assume their "natural values".  $E_v$  and  $E_\delta$ , the bond stretching and angle bending energies, respectively, result from stretching bonds and bending angles from their "natural values".  $E_t$ , the torsional energy, is associated with internal rotations, and  $E_{nb}$  is the energy of interaction between non-bonded atoms. Additional terms can be added to consider the occurrence of specific interactions like intramolecular hydrogen bonding or electrostatic interactions [13,15].

Experience has shown that the choice of functions in the force field is critical. In addition, while a variety of efficient and fast computational algorithms is widely available, the final force field should be both reliable and simple.

## Bond stretching and angle deformation

The most extensively used potential energy function associated with bond stretching is

$$V_v(b) = K_{1v}(b-b_0) + 1/2 K_{2v}(b-b_0)^2 + 1/6 K_{3v}(b-b_0)^3 \quad (2)$$

where  $b$  is the instantaneous bond length,  $b_0$  is the corresponding "natural" value and  $K_{1v}$ ,  $K_{2v}$  and  $K_{3v}$  are related with the "resistance" of the bond to stretching.

In general, the same kind of function is chosen to represent the potential energy change on angle deformation, *i.e.*,

$$V_\delta(\theta) = K_{1\delta}(\theta-\theta_0) + 1/2 K_{2\delta}(\theta-\theta_0)^2 + 1/6 K_{3\delta}(\theta-\theta_0)^3 \quad (3)$$

When both  $K_{1\alpha}$  and  $K_{3\alpha}$  ( $\alpha = v$  (stretching) or  $\delta$  (bending)) are chosen to be zero,  $\langle 2 \rangle$  and  $\langle 3 \rangle$  reduce to harmonic functions. This simplification is very useful from a practical point of view, as it considerably reduces the number of parameters and the computational time required. It has been followed thoroughly during the development of the **PF1/PF2** force fields.

Experience has demonstrated that the use of harmonic functions generally leads to significantly accurate results, though some studies have been presented that include other terms. In particular, linear terms have been considered [2,16], though their inclusion seems to

be redundant as it amounts to a redefinition of  $b_0$  or  $\theta_0$ . On the other hand, cubic terms deal with anharmonicity, at least in an approximate way. However, they lead to badly behaved functions for large displacements from the equilibrium position (Fig. 1). While this difficulty has been dealt with successfully [17,18], the practical advantages of including cubic terms are not much relevant.

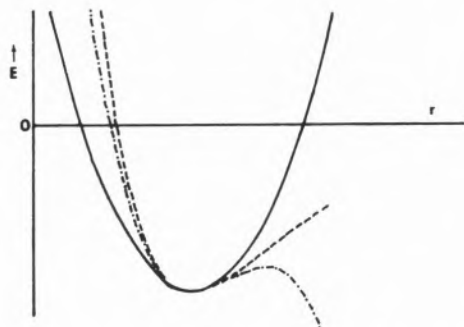


Figure 1 – Harmonic and anharmonic potential: —, harmonic potential; ---, Morse type potential – · – ·, harmonic with cubic term added

Another way to account for anharmonicity is to use Morse functions [19]. In particular, for bond stretching [20]

$$V_v(b) = D \exp[-2k(b-b_0)] - 2D \exp[-k(b-b_0)], \quad (4)$$

where  $D$  and  $k$  are related with the dissociation energy and the stretching force constant, respectively. While these functions present some theoretical advantages, the additional computational effort they give rise to discourages their use.

Angle bending terms are of fundamental importance to geminal interactions. The preference for a function like (3) results mainly from its simplicity. However, the inclusion of additional terms related with interactions between adjacent stretching and bending coordinates, have been proposed by several authors [21,22], the

$$V_{vv}(b,b') = 1/2 K_{vv}(b-b_0)(b'-b_0) \quad (5)$$

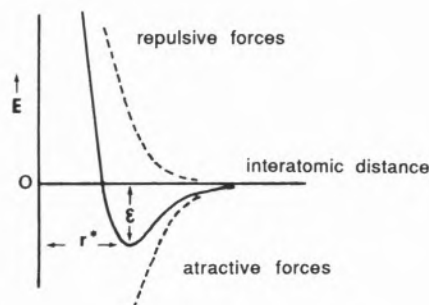
$$V_{v\theta}(b,q) = 1/2 K_{v\theta}(b-b_0)(\theta-\theta_0) \quad (6)$$

main objective being a better agreement between calculated and experimental vibrational frequencies. Our experience shows that the inclusion of such terms is neither essential to a good force field nor worth the effort.

### Non-bonded interactions

The quantitative treatment of intramolecular non-bonded interactions in MM relies very much on simple van der Waals interatomic potentials obtained from rare

gases studies [23]. The general form of these potentials exhibits a short distance repulsive interaction and a long distance attraction. The resulting potential profile can be characterised by the minimum energy distance,  $r^*$  (related with the van der Waals atomic radii), the height of the potential well  $\epsilon$  (connected with atomic polarizabilities), and the slope of the repulsive section of the curve.



The attractive part of the potential is due to the London dispersion interaction [24]. Perturbation theory yields the following general function

$$V_{\text{disp}}(r) = -C_1 r^{-6} - C_2 r^{-8} - C_3 r^{-10} - \dots \quad (7)$$

where  $r$  is the interatomic distance and  $C_1, C_2, C_3, \dots$  depend on atomic polarizabilities and ionization potentials [25]. At short distances, repulsive interactions of the orbital overlap and nuclear-nuclear types dominate, and are generally represented by a negative exponential function or by a positive inverse power function of the interatomic distance,

$$V_{\text{rep}}(r) = A \exp(-Br), \quad (8)$$

$$V_{\text{rep}}(r) = Ar^{-n}, \quad (9)$$

where  $A$  and  $B$  are adjustable parameters. The results obtained with these functions are qualitatively similar.

The potential functions most extensively used in MM for non-bonded interactions (1-4 and larger) are the modified Buckingham [26] and the Lennard-Jones [27] functions, which result from combining the first term of (7) with expressions (8) or (9), respectively:

$$V_{\text{nb}}(r) = A \exp(-Br) - Cr^{-6} \quad (10)$$

$$V_{\text{nb}}(r) = Ar^{-n} - Br^{-6} \quad (11)$$

In the case of Lennard-Jones functions, it is common practice to keep  $n$  as a constant (usually 12 or 9) [13-15], though its use as an adjustable parameter improves the quality of the results. While a slightly modified Buckingham potential with two parameters has also been used [28,29], experience shows that this reduction in the number of parameters leads to poor results [13], as

in the case of Lennard-Jones functions. Thus, a potential function with three adjustable parameters seems to be necessary for a good description of the van der Waals interactions. In both **PF1** and **PF2**, modified Buckingham potentials with three adjustable parameters are used.

The above mentioned non-bonded potentials assume spherically symmetric electronic densities on atoms and are insensitive to distinct atomic environments.

The first approximation does not work well for atoms with small atomic numbers as these display considerably asymmetric electronic distributions in a molecule. This is especially critical for the hydrogen atom whose single electron gets involved in a bond. In particular, when molecular geometries are correlated with X-ray geometries in crystals, van der Waals potentials centred off the hydrogen atom nuclei have been considered [29-32]. For isolated molecule studies, the choice of less repulsive potentials like those used in both **PF1** and **PF2** strongly improves the results [9,10] without any additional complication.

Atoms with electron lone pairs, like oxygen and sulphur, also display asymmetric electronic densities. Sometimes, the lone pairs have been successfully simulated by specific van der Waals potential functions [33] that picture them as pseudo-atoms. However, this approximation should be discouraged as the explicit consideration of electron lone pairs strongly increases the complexity of the potential energy function. In addition, recent studies clearly indicate that van der Waals lone pair potentials are not necessary, provided the force field optimization is carefully carried out [3,9-12].

The second approximation — insensitivity of non-bonded potentials to distinct atomic environments — is a crude representation of reality, especially when the interacting atoms have large polarizabilities like sulphur or chlorine atoms. In particular, this approximation does not distinguish between atoms on the same side of the molecular skeleton or on opposite sides when the interaction is significantly reduced by the shielding effect of the skeletal atoms. While theoretically unrealistic, this approximation has been assumed so far in all MM studies, and yields excellent agreement with experimental results.

Additional terms related with non-bonded interactions have also been frequently used, in particular, for the consideration of electrostatic interactions [13-15,34-37]. Though the inclusion of these terms was considered relevant by several authors, our experience shows that they can be ignored in a majority of cases, provided van der Waals potentials are correctly evaluated [9,10].

### Torsions

Torsional terms are essential for the development of a reliable MM force field, as they take into account interactions not explicitly considered in van der Waals terms, in particular, electronic exchange between adja-

cent bonds [13] (an alternative interpretation of their importance considers that torsional energy is related with van der Waals repulsion anisotropy, as this is clearly more important for small than for large dihedral angles [38]). In fact, while some effort has been dispensed by several authors to obtain a suitable force field without torsional terms [13-15], no success has yet been reached.

Torsional potentials are usually expressed as functions of the torsional angle (dihedral angle)  $\varphi$ , using a cosine type Fourier series,

$$V_{\tau}(j) = -\frac{1}{2} \sum_n K_{n\tau} [1 - \cos(n\varphi)] \quad (12)$$

where  $K_{n\tau}$  are related with rotational barriers and the expansion is truncated in consonance with the rotor symmetry. A frequent simplification, implemented in **PF1/PF2**, uses a single cosine function, *i.e.*, the first term of Eq. (12) for non-symmetrical rotors, and the  $n=3$  term for  $C_{3v}$  rotors. This simplification reduces considerably the number of potential parameters and does not originate qualitative changes in the results, thus being very useful from a practical point of view.

Essentially, there are two different ways for consideration of torsions in a mm calculation: *i*) one torsional angle per bond between chain atoms (group torsional model [39]) or, *ii*) one torsional angle for each combination of outer pairs of atoms around a bond (bond torsional model [40]). The second approximation is more appropriate for a nonsymmetrical arrangement of groups and is adopted in **PF1/PF2**.

Torsions around double or partially double bonds are associated with large energy barriers mainly due to electronic effects originated by the reduction of  $\pi$  overlap for non-planar conformations. As these torsional potentials present a maximum value for a dihedral angle near  $90^\circ$ , **PF1/PF2** force fields include a two-fold cosine function ( $n=2$  in expression (12)), with a negative value of  $K_{2\tau}$  to account for these specific electronic effects. While an additional  $n=4$  term has been already previously proposed to soften the resulting potential [41], its inclusion is not necessary and is not implemented in our force fields.

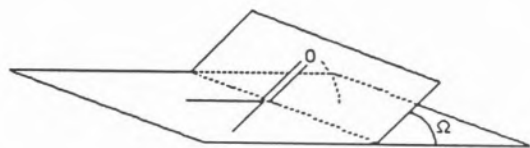
The harmonic function,

$$V_{\tau}(\varphi) = \frac{1}{2} K_{\tau} (\varphi - \varphi_0)^2, \quad (13)$$

where  $\varphi_0$  is the dihedral angle corresponding to the minimum energy conformation, was also proposed to represent the torsional potential around double bonds [14]. However, this potential may only be used near the energy minima, when good estimates of equilibrium geometries are available.

The out-of-plane wagging deformations ( $\Omega$ ) are considered as particular cases of torsion and in both **PF1** and **PF2**, this kind of interaction is represented by a cosine function of  $\Omega$  with  $n=1$ .





The inclusion of mixed terms involving torsional coordinates has also been suggested by several authors [21,42], to reach an improved agreement between calculated and experimental vibrational frequencies. However, these terms are not essential for the development of a good force field in the large majority of cases [9-15] and have not been considered in **PF1** or **PF2**.

### Force field parameterization

The choice of the potential terms is not the single degree of freedom from which the final quality of the force field depends. All potential functions contain interdependent parameters (Fig. 2) which have to be determined as a set, as individual values are not physically meaningful. The optimization process improves on an initial parameter set, until calculated and experimental values agree within predetermined precision.

Stretching:

$$V_v = \frac{1}{2} K_v (b - b_0)^2$$



Bending:

$$V_\delta = \frac{1}{2} K_\delta (\theta - \theta_0)^2$$



Torsion:

$$V_\omega = \frac{1}{2} K_\omega (1 + \cos(n\varphi))$$



Out-of-plane wagging:

$$V_\tau = \frac{1}{2} K_\tau (1 + \cos(\Omega))$$



Non-bonded:

$$V_{nb} = A e^{-B r} - \frac{C}{r^6}$$



Figure 2 – Potential functions selected to build **PF1**/**PF2** molecular mechanics force fields. Force field parameters are printed in bold-type

The optimization process can be carried out automatically or by direct inspection of the results. Automatic optimization methods are essentially based on a least squares algorithm that solves the system of

$n_{\text{opt}}$  simultaneous equations where  $n_{\text{opt}}$  is the total

$$\partial \mathbf{y}^2 / \partial k_n = 0 \quad n = 1, \dots, n_{\text{opt}} \quad (14)$$

number of potential parameters,  $k_n$  refers to the  $n^{\text{th}}$  parameter to optimize and  $\mathbf{y}$  is the difference vector between experimental and calculated values.

The basic difficulty of this optimization procedure lays on establishing a reliable method of weighting the various molecular properties [15], as parameterization requires a large number of distinct molecular properties. Geometries, conformational energies and thermodynamic properties are generally used; less frequently, vibrational frequencies, dipole moments, magnetic properties or rotational constants are also considered.

The classical least squares minimization method assumes a linear Taylor expansion:

$$\mathbf{y}_{(i+1)} = \mathbf{y}_{(i)} + \sum_{n=1, n_{\text{opt}}} (\partial \mathbf{y} / \partial k_n) dk_n \quad (15)$$

This is a reasonable approximation providing the initial estimates of the parameters are good. The derivatives in expression (17) are calculated in part analytically, since the computing time for a pure numerical evaluation becomes prohibitive [15].

It is important to recall that the convergence of the optimization process is strongly dependent on the initial parameter estimates, thus calling for an active human participation. Therefore, the combined use of the automatic and by-direct-inspection optimization procedures is likely to yield a better parameterized force field [10], thus being used thoroughly in the **PF1** and **PF2** parameterizations.

Whatever the optimization method is, a force field parameterization is always an extremely complex process as it requires a judicious choice of model compounds and observables and involves a large amount of varied experimental data.

It should be pointed out that different experimental techniques yield geometries with different physical meanings, even when the samples are in the same phase. As the development of a force field for isolated molecules requires experimental data from the gaseous phase, the most widely used experimental techniques are microwave spectroscopy and electron diffraction. Since these two techniques are based in different physical phenomena, it is not surprising that they yield non-equivalent structures [43,44]. In particular, as the interaction times for these experiments are different, vibrational motions affect the final structure in different ways. Therefore, the selection of a particular type of molecular structure for force field parameterization should be judiciously performed. As the high resolution power of microwave spectroscopy leads to molecular geometries most suitable for mm calculations they have been used systematically in **PF1** and **PF2**.

## Energy minimization

Once the force field is parameterized, it can be applied to a particular molecule to get the geometries of its conformations that correspond to minima in the potential energy surface.

The first MM studies could not calculate accurate equilibrium geometries. The geometries of the various conformations to be studied had to be supplied as data, and approximated equilibrium conformations were determined by varying systematically the relevant internal coordinates, one by one. These limitations were overcome after the development of a mathematical algorithm based on an iterative procedure, to perform automatic minimization of the "steric" energy [40].

The analytical solution of the minimization problem is too complex as it requires the solution of a system of  $n_{\text{cord}}$  non-linear equations

$$\partial E / \partial x_n = 0 \quad n = 1, \dots, n_{\text{cord}} \quad (16)$$

where  $x$  represents the coordinates in the configurational space of the molecule. Therefore, the minimization is carried out using numerical methods. Among these, the gradient search methods are the most widely used.

The first minimization method used in MM [40] was based in the steepest descent algorithm [45]. This algorithm is quite efficient during the initial minimization steps, far from the minimum, but it leads to a rather slow convergence near the bottom of the potential well. Therefore, the method is now generally used in the initial stages of the minimization process, and is followed, closer to the equilibrium positions, by methods based in more efficient algorithms, like the Newton-Raphson [46] or the Davidon-Powell-Fletcher [47,48] algorithms.

All methods minimize a given input geometry to a local minimum in the potential energy surface. For molecules with more than a single minimum, the final structure depends on the input geometry. Thus, the conformational analysis of a molecule often requires multiple optimizations, starting with input geometries in different regions of the potential energy surface. In addition, the final geometry depends also on the termination criterium used to stop the iterative process. The most widely used criteria are based on the proximity, to a small predetermined value, of an energy or a geometry variation in subsequent steps. However, when the potential energy well near the minimum is very broad, both of these criteria may stop the minimization process before an acceptable energy minimum has been reached. To avoid this problem, the precision of the termination criterium could be increased, though to the expenses of computational time. A more efficient termination criterium, used in our calculations, is based on the fact that the energy gradient should vanish for equilibrium conformations, and the minimization procedure

is stopped when the quadratic norm of the energy gradient reaches a value sufficiently close to zero.

Sometimes, in a MM calculation, the energy minimization process can lead to a false minimum or to a saddle point. False minima result either from an inadequate minimization technique or from a less realistic parameterization of the force field. Saddle points satisfy the criteria imposed by minimization algorithms, namely the annulment of the energy gradient. However, both of these problems can be avoided if a systematic study of the conformational behaviour of the molecule near each point resulting from minimization is carried out, and adequate algorithms and termination criteria are used [9-14].

## Molecular properties calculation

The fundamental ideas of MM are centred on two expressions, namely, [1], which builds the potential energy of the molecule from various contributions, and the following Taylor expansion which allows to

$$E(\underline{x}) = E(\underline{x}_0) + \sum (\partial E / \partial x_i)_0 dx_i + \sum (\partial^2 E / \partial x_i \partial x_j)_0 dx_i dx_j \quad (17)$$

extrapolate to a neighbouring point the mathematical information on a particular point of the energy surface.

The first term represents the equilibrium "steric" energy of the molecule. Its physical meaning depends on the potential functions used to build the force field. The second term corresponds to the energy gradient and is zero for equilibrium conformations. The third term represents the harmonic vibrational energy, the partial derivatives being the harmonic force constants that define the vibrational force field for a particular equilibrium molecular conformation.

It is important to note the essential difference between potential parameters like  $K_{2v}$  or  $K_{28}$  (see equations (2) or (3)) and the vibrational force constants. In MM, the vibrational force field for each stable molecular conformation is defined and numerically evaluated from equation (17). On the other hand, all conformations of a given molecule are calculated using the same potential energy function, where several potential parameters are included.

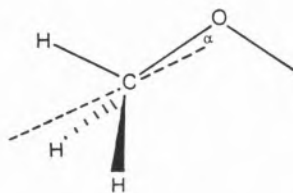
Once the force field is determined, it is easy to evaluate normal modes and their frequencies using one of the current methods of normal coordinate analysis. Wilson's method [49] solves the vibrational problem in internal coordinates; Gwinn's formulation [50] performs the calculations in cartesian coordinates. While Wilson's method is generally preferred by vibrational spectroscopists, mm vibrational calculations are usually performed following Gwinn's method as this requires only one matrix diagonalization and allows a checking of the energy minimization to be made. In fact, if the molecular geometry corresponds to a true minimum in the potential energy surface, six frequencies (five for

linear molecules) are equal to zero as they refer to rotational and translational motions. Once an equilibrium geometry is determined, other molecular properties like inertia moments and rotational constants can be calculated, and thermodynamic properties evaluated from vibrational frequencies and statistical considerations [51]. Infrared intensities can also be estimated provided electrostatic terms are included in the potential energy function.

## Alcohols and ethers

The force field for these families of molecules was parameterized using 19 model compounds (9 alkane and 10 alcohol and ether molecules) [3]. The inclusion of alkanes in the parameterization was necessary to deal with hydrocarbon fragments more accurately, and the results on this class of molecules can be found in refs. 3 and 10. In this case, as well as for alcohols and ethers, the results obtained with the **PF1** force field are in excellent agreement with the available experimental values and generally improve on existing calculated literature values.

The structure of the methanol molecule shows a small methyl tilt (angle  $\alpha$  of the C-O bond axis with the axis of rotation of the methyl group) towards the lone electron pairs of the oxygen atom [52,53].



Similar tilt angles have also been experimentally observed in other molecules, like dimethyl ether [54] or ethylmethyl ether [55] which also have a methyl group directly bonded to an oxygen atom. This general trend is correctly predicted by our calculations as all the calculated structures for the above considered molecules present small methyl tilt angles towards the oxygen lone electron pairs in good quantitative agreement with those observed experimentally [3,10].

The results of **PF1** MM calculations are also very useful for understanding and systematizing the general conformational preferences exhibited by both the C-C-O and C-C-O-X (X= H or C) axes in alcohols and ethers. In these molecules, the calculations indicate that both the C-C-C-O and C-C-O-X axes adopt preferentially the *anti* conformation (corresponding to a dihedral angle of 180°) [3,10]. A *gauche* C-C-O-C axis (dihedral angle equals  $\pm 60^\circ$ ) is destabilized by  $\approx 6$  kJ mol<sup>-1</sup> relatively to the most stable conformation, while a *gauche* C-C-C-O axis is destabilized only by  $\approx 2$  kJ mol<sup>-1</sup> relatively to the *anti* C-C-C-O axis in both alcohol and ether molecules

(Fig.3). This increase in the energy difference between *gauche* and *anti* conformations going from the C-C-C-O axis to the C-C-O-C axis relates with the stronger hydrogen-hydrogen interactions involving the hydrogen atoms directly bonded to the terminal carbon atoms in this latter case. The energy difference between the two stable conformations of the C-C-O-H axis (*anti* and *gauche*) is very small ( $\approx 0.5$  kJ mol<sup>-1</sup>; see Fig.3).

The similarity observed in the calculated  $E_{g-a}$  values for ethers and alcohols indicates that internal rotation around the C-C central bond of this axis is not significantly affected by the group which is bonded to the oxygen atom.

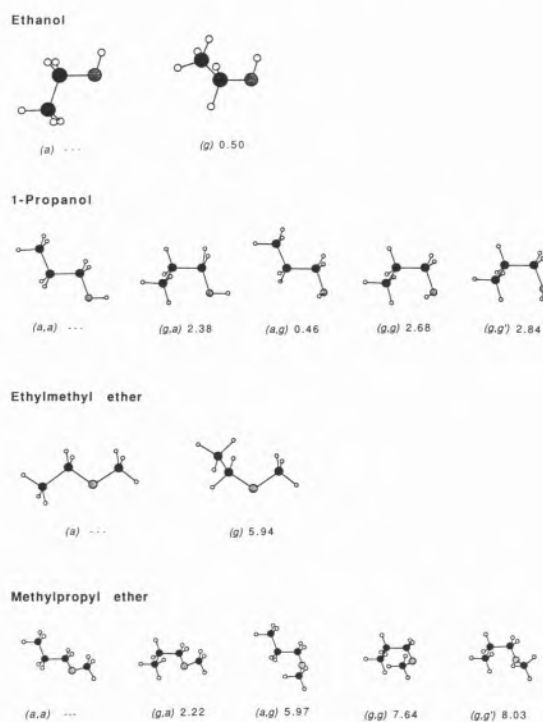


Figure 3 – Conformers and **PF1** relative energies (kJ mol<sup>-1</sup>) of 1-propanol, ethylmethyl ether and methylpropyl ether. g. *gauche*; a. *anti*.

During the **PF1** force field parameterization, we emphasized the importance of a general agreement between calculated and observed vibrational frequencies. In fact, MM cannot compete with traditional vibrational analysis without requiring an extraordinary increase in both the complexity of the force field and the number of potential parameters [10,14]. Nevertheless, the results obtained for this property with the **PF1** force field show a very good general agreement with the experimental values (Fig.4), the largest errors appearing, as expected, for methyl vibrations, considering the higher symmetry of this group (see ref.10 for detailed discussion).

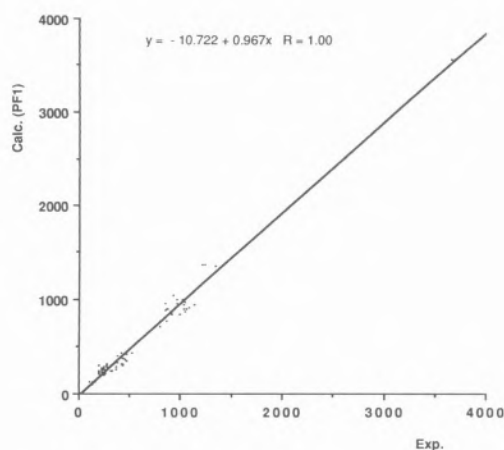


Figure 4 – Calculated (**PF1**) versus experimental vibrational frequencies ( $\text{cm}^{-1}$ ) for alcohol and ether molecules. Data was taken from refs. 3, 10 and references therein.

## Carbonyl compounds

The quality of the **PF1** results (structures and energies) for carbonyl compounds [4-6,10] is quite similar to that of the results obtained for alkanes, alcohols and ethers. In addition, experimental vibrational frequencies are generally better reproduced by the calculations in the case of carbonyl compounds, as discussed elsewhere [10].

We have used 17 molecules for the carbonyl force field parameterization, 3 of which are  $\alpha$ -chloro substituted compounds. While the results for these compounds are particularly interesting, they have been reviewed elsewhere [9], and thus will not be considered in this article.

In general, the calculated structures for aldehydes and ketones [10] agree very well with experiment, and improve existing calculated literature values [56]. In consonance with quantum-mechanical *ab initio* molecular orbital calculations [57], the **PF1** MM calculations indicate that aldehyde fragment behaves like a relatively rigid structural unit with respect to conformational changes. In fact, it was shown that both the aldehyde C-H and C=O bond lengths and the O=C-H bond angle do not change appreciably with the conformation [10]. On the other hand, the  $\text{C}_\beta\text{-C}_\alpha\text{-C}(=\text{O})$  bond angle in these compounds, as well as in ketones, are significantly dependent on the conformation adopted by the molecule. For instance, in propanal and 2-butanone, this angle decreases by  $\approx 1$  and  $\approx 2$  degrees, respectively, when the conformation changes from the most stable *syn* forms (with a C-C-C=O dihedral angle of  $0^\circ$ ) to the *skew* forms (with C-C-C=O dihedral angles in the  $\pm 120^\circ$  region). The larger C-C-C angle observed for *syn* forms can be ascribed, at least partially, to steric repulsions

operating between carbonyl oxygen lone electron pairs and the  $\beta$ -methyl groups.

The MM results obtained for 2-pentanone and 3-pentanone molecules are particularly useful to determine relative stabilities of conformations differing by internal rotation around  $\text{C}_\alpha\text{-C}(=\text{O})$  and  $\text{C}_\beta\text{-C}_\alpha$  single bonds in saturated ketones. 2-pentanone can exist in five distinct conformers (see Fig. 5, also for naming), the most stable one being the planar (*anti,anti*) form, with both  $\text{C-C-C}_{\text{sp}^2}\text{-C}$  and  $\text{C-C-C-C}_{\text{sp}^2}$  dihedral angles equal to  $180^\circ$ . A similar form — planar (*anti, anti*) — was also found to be the most stable conformers of 3-pentanone (see Fig.6). In fact, from our results for aliphatic ketones, it is possible to conclude that the molecular conformations having a *gauche* C-C-C<sub>sp<sup>2</sup></sub>-C axis are destabilized by approximately  $4 \text{ kJ mol}^{-1}$  relatively to those conformations having an *anti* C-C-C<sub>sp<sup>2</sup></sub>-C axis (Fig.5,6). In addition, the energy difference between a *gauche* and an *anti* C-C-

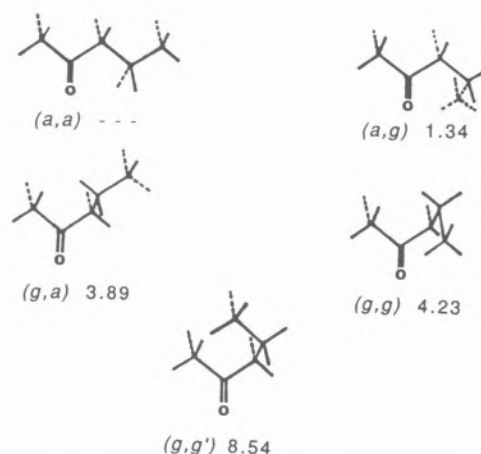


Figure 5 – Conformers and **PF1** relative energies ( $\text{kJ mol}^{-1}$ ) of 2-pentanone. g. *gauche*; a. *anti*

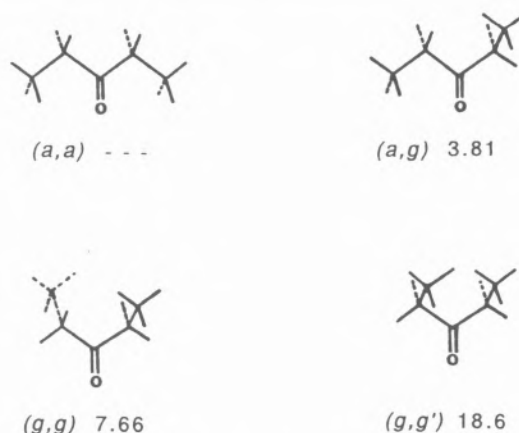
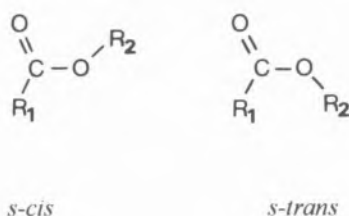


Figure 6 – Conformers and **PF1** relative energies ( $\text{kJ mol}^{-1}$ ) of 3-pentanone. g. *gauche*; a. *anti*



C-C<sub>sp2</sub> axis is  $\approx 1$  kJ mol<sup>-1</sup>, the *anti* form being the most stable one (see Fig.5). We should point out that the  $E_{g-a}$  in saturated ketones is significantly smaller than the *g-a* energy difference observed in the case of butane ( $\approx 4$  kJ mol<sup>-1</sup> [58]). This is certainly due to the fact that the H...H repulsive interactions that occur in the *gauche* forms of ketones are reduced by substitution of one of the methyl terminal groups of butane by the carbonyl linkage.

The internal rotation around the central C<sub>sp2</sub>-O bond in carboxylic acids and esters originates two different planar conformations the *s-cis* form, with a O=C-O-R dihedral angle equals to 0°, being more stable than the *s-trans* form (O=C-O-R dihedral angle equals to 180°).



Considering only intramolecular electronic effects, the energy maximum of the *s-cis*→*s-trans* interconversion reaction should occur for a O=C-O-R dihedral angle near 90°, when mesomeric delocalization reaches a minimum. While electronic effects are usually very difficult to account for by MM calculations, **PF1** force field proved to be very reliable to describe such kind of effects in carboxylic molecules [6,10,51]. Two illustrative examples of capital importance in conformational analysis of these compounds can be pointed out:

i) It is known that the mesomeric delocalization  $O=CR-OR' \leftrightarrow O-CR=OR'$  is less important in the *s-trans* forms of carboxylic acids and esters than in their most stable *s-cis* forms [9-11,59]. This different stability reflects itself in the values of structural parameters, like C-O bond lengths. In particular, **PF1** calculations predict that the central C-O bond length increases by a few picometers and the C=O bond length reduces slightly when going from *s-cis* to *s-trans* conformers [3-6,10], in agreement with experiment.

ii) The **PF1** calculated energy differences between *s-trans* and *s-cis* conformers in acetic acid and its methyl ester increase by approximately 8 kJ mol<sup>-1</sup> in the latter molecule [4]. In addition, in methyl acetate, this barrier is predicted to be greater than in acetic acid by  $\approx 20$  kJ mol<sup>-1</sup> [4]. Also, the maximum of the barrier does not seem to occur at 90° in methyl acetate, as it should be predicted if only mesomeric effects were operating in the O=C-O group, but at *ca.* 100°. These increments in the energy differences and in the angle of maximum potential energy may be ascribed both to steric repulsion between the acetyl and methoxyl groups and to the larger inductive or hyperconjugative effect of the methyl ester group. It is remarkable that **PF1** can account for such kind of conformational features, even when both

steric and electronic effects are operating simultaneously.

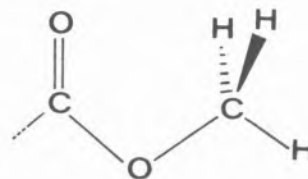
From the MM results it can be concluded that the (*s-trans*)-(*s-cis*) energy differences in simple saturated aliphatic carboxylic acids and esters are  $\approx 25$  and  $\approx 35$  kJ mol<sup>-1</sup>, respectively (exceptions to this general rule are HCOOH and HCOOCH<sub>3</sub>). In addition, the energy barriers for *s-cis*→*s-trans* isomerization are  $\approx 45$  kJ mol<sup>-1</sup> in carboxylic acids and  $\approx 65$  kJ mol<sup>-1</sup> in esters.

The relative stabilities of conformations differing by internal rotation around C<sub>α</sub>-C and C<sub>β</sub>-C<sub>α</sub> bonds in carboxylic acids and esters were also examined and proved to be qualitatively similar to those observed for aldehydes and ketones. Thus, in these molecules, the C-C-C=O and the C-C<sub>β</sub>-C<sub>α</sub>-C axes adopt preferentially *syn* and *anti* forms, respectively. The less stable *skew* C-C-C=O conformations are higher in energy by  $\approx 6$  kJ mol<sup>-1</sup> than the *syn* forms; the *gauche* C-C<sub>β</sub>-C<sub>α</sub>-C conformers are  $\approx 4$  kJ mol<sup>-1</sup> less stable than the *anti* form. It is interesting to note that, in both cases, the energy differences between the less stable (*skew* or *gauche*) forms and the most stable form are higher than those found in ketones.

The results obtained for acyl chloride molecules show that a *syn* C-C-C=O axis in these compounds corresponds also to the most stable form, *skew* forms yet being  $\approx 6$  kJ mol<sup>-1</sup> higher in energy than the *syn* conformer [10].

Conformational preferences of the ester group can be summarized as follows:

i) In methyl esters, the lowest energy conformation is the *anti* form, with a H-C-O-C dihedral angle of 180°. In the *syn* conformation (energy maximum) there is a strong steric interaction between the carbonyl atom and the methoxy hydrogen atom (in the plane) that reflects on the large calculated O-C-H<sub>in-plane</sub> angles found for this conformation [4].



ii) The internal O-C barrier of rotation of the methyl ester group is  $\approx 5$  kJ mol<sup>-1</sup> for all compounds studied in the O=C-O-C *s-cis* conformation. This energy barrier strongly increases for *s-trans* O=C-O-C forms due to the proximity of the methyl ester and the acyl groups.

iii) The C-O-C-C internal rotation in ethyl ester molecules originates two different stable conformers, the *anti* form (dihedral angle of 180°) being most stable than the *gauche* form (C-O-C-C dihedral angle  $\approx 80^\circ$ ) by  $\approx 1$  kJ mol<sup>-1</sup>.

**PF1** vibrational results on carbonyl compounds are summarized graphically in Fig.7. As it was pointed

out before, the MM vibrational results for these molecules are in better agreement with the experimental values than in the case of alkanes, alcohols and ethers. This is because the reduced symmetry of the carbonyl moiety makes each calculated frequency essentially dependent on the value of a single potential parameter. In more symmetrical groups, one single parameter may be important to determine the calculated values for several vibrations.

Figure 7 makes clear that the worse agreement obtained between calculated and experimental frequencies occurs for C-C stretching modes. This can be easily understood considering the high degree of vibrational coupling usually found for these vibrations, as well as their sensitivity to structural changes.

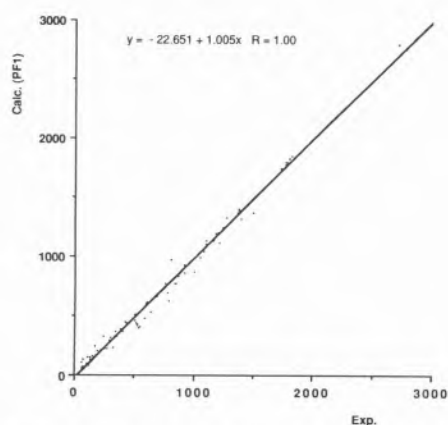


Figure 7 – Calculated (**PF1**) versus experimental vibrational frequencies ( $\text{cm}^{-1}$ ) for carbonyl molecules. Data was taken from refs. 3, 10 and references therein.

## Thiols and thioethers

The force field for thiols and thioethers (**PF2**) was developed using 9 representative molecules (5 thiols and 4 thioethers) [11]. **PF1** force field parameters were used to deal with hydrocarbon molecular fragments.

The calculated values and the available experimental data for these classes of compounds are in good general agreement. In opposition to what was observed in the case of alcohols and ethers, the MM calculations show that a methyl group directly bonded to the sulphur (thiol or thioether) atom does not show any important tilt towards the sulphur lone electron pairs. The absence of such structural feature in these molecules can be partially ascribed to the longer C-S bond length.

The results obtained for 1-propanethiol are particularly relevant to the understanding of conformational preferences of both the C-C-C-S and C-C-S-H axes in thiols. We have calculated the structures and relative energies of the five expected conformers, *ag*, *aa*, *gg*, *gg'* and *ga* of this molecule (Fig.8). In this notation, the first letter refers to the conformations around the C-C bond,

and the second to the conformations around the C-S bond. The C-C *anti* forms have been determined to be more stable by  $\approx 1.7 \text{ kJ mol}^{-1}$  than the forms which have a C-C *gauche* conformation. The calculated bond lengths and angles in the various conformers are similar. However, the C-S and C-C central bonds as well as the C-C-S angle are slightly increased in the *gauche* C-C forms [11], thus indicating some intramolecular strain in these conformers.

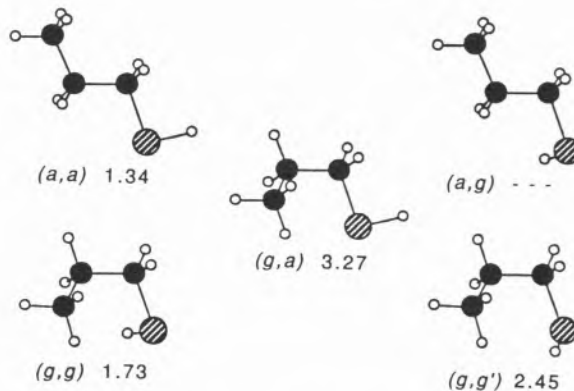


Figure 8 – Conformers and **PF2** relative energies ( $\text{kJ mol}^{-1}$ ) of 1-propanethiol. *g*, *gauche*; *a*, *anti*.

In all studied molecules the sulphydryl group adopts preferentially a *gauche* position (see Fig.8); the *anti* form is higher in energy than the *gauche* form by  $\approx 1.3 \text{ kJ mol}^{-1}$ . It should be pointed out that this conformational trend contrasts with that observed in the case of the oxygen analogue molecules which have *anti* C-C-O-H axes more stable than *gauche* C-C-O-H axes, as it was already mentioned in this article. This distinct conformational behaviour seems to suggest that longer C-S bond lengths — leading to longer non-bonded H...H distances and to reduced steric hindrance in *gauche* conformations — might be the origin of this conformational preference around the C-C-S-H axis.

The *gauche* arrangement preference in the immediate neighbourhood of a sulphur atom seems to be a general trend, as the MM calculations also predict that the most stable C-C-S-C axis conformation in thioether compounds is also *gauche* [11]. The results of the calculations on ethylmethyl, methylpropyl and diethyl sulphide molecules are particularly interesting on this instance. The relative stability of the *gauche* and *anti* conformers of ethylmethyl sulphide have been the subject of a variety of experimental and theoretical studies. Experimental work on this molecule has included vibrational spectroscopy [60-65], electron diffraction [66] and microwave spectroscopy [67,68]. It was believed at one time that the *anti* form was more stable than the *gauche* form, and an older MM force field [69] predicted the *anti* form to be  $1.21 \text{ kJ mol}^{-1}$  lower in energy than the *gauche* conformer. However, an *ab initio*

SCF MO calculation with a 3-21G+d (C,S) basis set and a second order Moller-Plesset perturbation correction to include electron correlation led recently to the conclusion that the *gauche* form is the most stable [70]. This conformational preference is well reproduced by our MM force field, with the *gauche* conformer calculated to be 0.7 kJ mol<sup>-1</sup> more stable than the *anti* form (Fig.9). In addition, **PF2** indicates that the most stable conformers of diethyl sulphide and methylpropyl sulphide molecules are the *gg* and *ag* forms, respectively (in the case of methylpropyl sulphide, the notation assigns the first letter to the conformation of the C-C-C-S axis and the second to the conformation of the C-C-S-C axis).

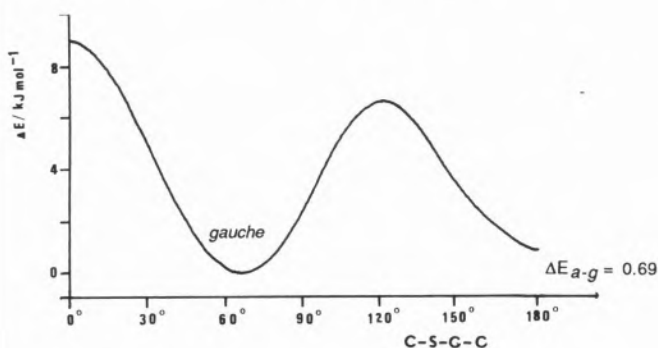


Figure 9 – **PF2** potential energy profile for internal rotation about the C-S bond in ethylmethyl sulphide, showing the greater stability of the *gauche* conformer as compared with the *anti* form.

It is interesting to note that the relative stability of an *anti* and *gauche* C-C-X-C axis (X= C, O, S) favours more the *anti* form for X=O than for X=C, and is reversed for X=S, the *gauche* form being the most stable in this case. A plot of  $E_{g-a}$  vs. C-X bond length gives a straight line (Fig.10) thus showing that the *g-a* relative stability

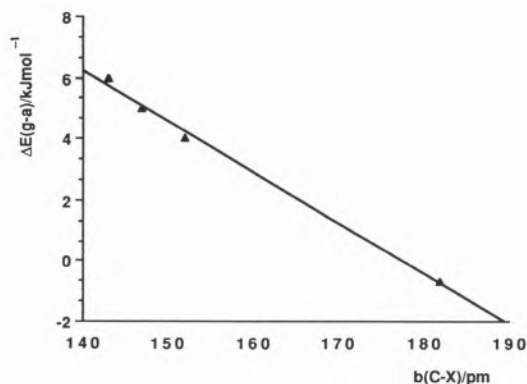


Figure 10 –  $\Delta E_{g-a}^{calc}$  (X= O, CH<sub>2</sub>, NH, S) versus the length ( $b_{C-X}$ ) of the C-X central bond. The straight line obeys to the equation  $\Delta E_{g-a}^{calc} = 29.61.b_{C-X} - 0.17$ , the correlation coefficient being 1.00.

around a C-C-X-C axis depends on the length of the central C-X bond. We should recall that the data presented in Fig.10 also include recent results on relative energies of *gauche* and *anti* forms of the C-C-N-C axis in ethylmethyl amine [71], and that the linear dependence observed for the above considered molecules is also obeyed by this molecule.

**PF2** vibrational results on thiols and thioethers are summarized in Fig.11. This Figure presents only the results for skeletal vibrations and for those modes involving the functional groups. The calculated values for other modes show the same general trends found for alkane, alcohol and ether molecules. Generally speaking, the agreement between calculated and experimental values is satisfactory, while the calculated C-C stretching frequencies are too small, a trend which had already been noticed for alkanes [3].

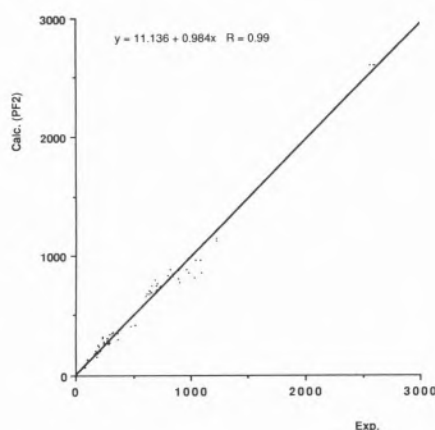


Figure 11 – Calculated (**PF2**) versus experimental vibrational frequencies (cm<sup>-1</sup>) for thiol and thioether molecules. Data was taken from refs. 10, 11 and references therein.

## Thiocarbonyl compounds

The most recent extension of **PF2** to thiocarbonyl compounds was intended to deal with thioaldehyde, thione, dithioacid and dithioester groups. Ten model compounds were used to determine specific thiocarbonyl potential parameters. The resulting force field is the first MM force field parameterized for these families of molecules. In fact, the necessary information for such force field development only recently became available, as a result of our investigations on the structures and properties of thiocarbonyl compounds by means of a series of systematic *ab initio* quantum mechanical SCF-MO calculations [10,59,72-74].

The MM results obtained for the molecules used in the parameterization agree very well with the reference *ab initio* values [10-12]. In addition, changes in molecular geometries associated with internal rotations are also

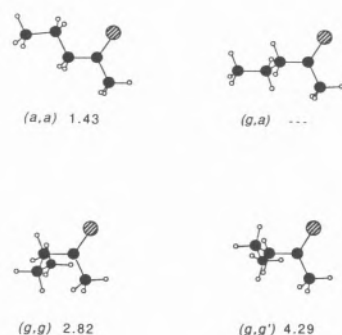
correctly predicted. For instance, the **PF2** calculated C=S and C-C<sub>sp2</sub>-H angles for ethanethial in the *anti* conformation (H-C-C=S dihedral angle equals to 180°) are 125.3° and 116.2°, respectively; the *ab initio* values for these angles are 125.0° and 116.2°. In addition, in the lowest energy conformation (*syn*), these angles (*ab initio* ; **PF2**) are (125.6° ; **126.7°**) and (115.5° ; **115.4°**), respectively, while the H-C=S angles were predicted to be very similar in both conformations, by mm as well as by *ab initio* methods. Molecular mechanical calculations predict also correctly the relative values of C-H bond lengths and C<sub>sp2</sub>-C-H angles involving the hydrogen atoms located in and out of the molecular plane. Molecular orbital calculations [74] have shown that the  $\alpha$ -carbon 2s orbital has a larger contribution to the C-H in-plane bond than to the out-of-plane bonds. The larger s character of the in-plane bond leads to a relatively small bond length for this bond and to a larger C<sub>sp2</sub>-C-H angle.

The conformational study of 2-pentanethione and 3-pentanethione is particularly relevant to the understanding of conformational preferences exhibited by C-C-C<sub>sp2</sub>-C and C-C-C-C<sub>sp2</sub> axes in the vicinity of a thiocarbonyl group. In consonance with the relative stability of the

various conformers of these molecules (Fig.12), a *gauche* C-C-C<sub>sp2</sub>-C axis ( $\pm 60^\circ$ ) is more stable than an *anti* C-C-C<sub>sp2</sub>-C axis (180°) by approximately 1kJ mol<sup>-1</sup>. This contrasts with the trends exhibited by carbonyl compounds where the *anti* conformation is the most stable one. On the other hand, the C-C-C-C<sub>sp2</sub> axis adopts preferentially the *anti* conformation, either in thiocarbonyl or in carbonyl compounds. However, the C-C-C-C<sub>sp2</sub> *gauche-anti* energy difference is appreciably larger in thiocarbonyl than in carbonyl molecules ( $E_{gauche-anti} \approx 3$  and 1 kJ mol<sup>-1</sup>, respectively). This destabilization of *gauche* forms upon O→S substitution results mainly from strong interactions between the sulphur atom and the *gauche* 3-methyl substituents due to the larger van der Waals radius of the sulphur atom.

Geometry changes accompanying the *s-cis*→*s-trans* conversion in dithioacids and dithioesters (see refs. 72 and 73 for a detailed discussion) are correctly predicted

#### 2-Pentanethione



#### 3-Pentanethione

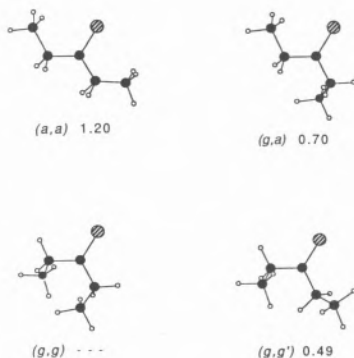


Figure 12 – Conformers and **PF2** relative energies (kJ mol<sup>-1</sup>) of 2-pentanethione and 3-pentanethione. *g*, *gauche*; *a*, *anti*.

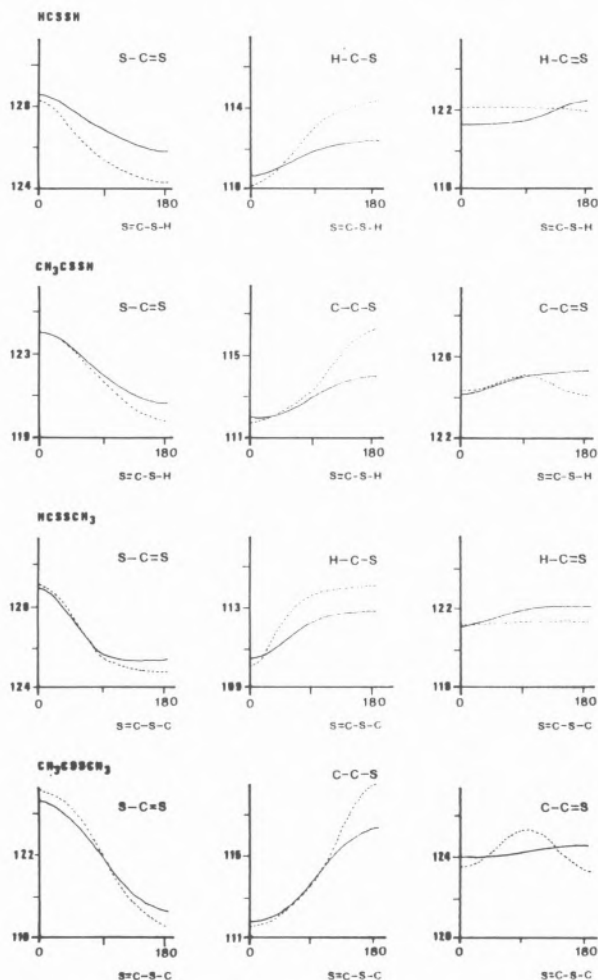


Figure 13 – Geometry changes accompanying the *s-cis*→*s-trans* conversion in RC(=S)SR (R = H or CH<sub>3</sub>) molecules, —, **PF2**—, *ab initio* 3-21G.



by the MM calculations. Figure 13 shows an excellent agreement between MM and *ab initio* results for S=C-S, X-C=S and X-C-S angles (X=H or C) of dithioformic and dithioacetic acids and their methyl esters, along the *s-cis*→*s-trans* isomerization.

The results obtained for the set of molecules having one  $\alpha$ -methyl group ( $\text{CH}_3\text{CH}_2\text{C}(=\text{S})\text{X}$ , X= H,  $\text{CH}_3$ , SH or  $\text{SCH}_3$ ) enable us to correlate conformational preferences of this group with the X substituent. In all the molecules studied *gauche* forms are more stable than *syn* forms, the C-C-S dihedral angles of the *gauche* forms increasing along the series X= H ]  $\text{SCH}_3$  (*s-cis*)  $\approx$  SH (*s-cis*) ] SH (*s-trans*)  $\approx$   $\text{SCH}_3$  (*s-trans*). Considering that larger C-C-S angles correlate with smaller  $\text{CH}_{3(\alpha)}\dots\text{X}$  distances and stronger  $\text{CH}_{3(\alpha)}\dots\text{X}$  repulsive interactions, the calculated values of these angles in the above series of molecules show that  $\text{CH}_{3(\alpha)}\dots\text{X}$  interactions are more important when the X substituent is bulky and positively charged. These interactions destabilize *gauche* forms with respect to the *syn* conformer, reflecting on the largest *gauche-syn* energy differences for molecules where X is a methyl group, or for molecules that exhibit a *s-trans* conformation around the C—S central bond.

The results obtained for molecules having two  $\alpha$ -methyl groups ( $\text{C}(\text{CH}_3)_2\text{HC}(=\text{S})\text{X}$ , X= H,  $\text{CH}_3$ , SH and  $\text{SCH}_3$ ) reveal that a similar correlation between conformational preferences and the nature of the X group can also be established for these molecules. In this case, bulkier and more positive X groups correlate with less stable *syn* forms, because in this conformation both  $\alpha$ -methyl groups are placed near the X group. Thus, the *syn* form is the most stable form when X = H, SH(*s-cis*) and  $\text{SCH}_3$ (*s-cis*), while the *gauche* form becomes the most stable one either for the *s-trans* forms of the dithioacid and dithioester molecules or for X =  $\text{CH}_3$ .

As it was shown for single methyl substituted molecules, the calculated relative values for the H-C-C=S dihedral angle of the *gauche* forms can also be used to analyse the relative strength of the  $\text{CH}_{3(\alpha)}\dots\text{X}$  interactions along the series of molecules now considered, though, in this case, larger H-C-C=S dihedral angles correspond to larger  $\text{CH}_{3(\alpha)}\dots\text{X}$  distances.

The results obtained for ethyl dithioesters allow to understand the conformational preferences of the ethyl fragment in these molecules. In both ethyl dithioformate and ethyl dithioacetate the internal rotation around the C-S bond gives rise to two distinct stable conformations: the *anti* (C-C-S-C dihedral angle equals  $180^\circ$ ) and the *gauche* forms (C-C-S-C dihedral angle near  $60^\circ$ ). The lowest energy forms, for both *s-cis* and *s-trans* S=C-S-C axes, correspond to the *gauche* form, in contrast to the dioxygen compounds. These conformational preferences can be explained considering:

i) the larger C-S bond lengths that result in weaker  $\text{CH}_3(\text{gauche})\dots\text{S}=\text{S}$  steric interactions in dithioesters compared to  $\text{CH}_3(\text{gauche})\dots\text{O}=\text{O}$  interactions in oxygen esters;

ii) the reduced mesomeric aptitude of the sulphur

atom, leading to a less effective electronic stabilization of the *anti* conformer in dithioesters than in esters;

iii) the stronger through-space repulsive interactions between thiolic lone electron pairs and the terminal methyl group (more important in the *anti* conformer than in the *gauche* form), as compared with  $\text{CH}_3\cdots\text{O}_{\text{lone pairs}}$  interactions in oxygen esters.

In consonance with the above reasoning, the  $\text{C}_{\text{sp}^2}\text{-S-CH}_2\text{-CH}_3$  axis should also preferentially adopt the *gauche* conformation in ethyl thioesters, while the lowest energy conformation of the  $\text{C}_{\text{sp}^2}\text{-O-CH}_2\text{-CH}_3$  axis in ethyl thionoesters should be *anti*.

PF2 vibrational results on thiocarbonyl compounds are resumed in Fig.14, where they are compared with experimental data. It can be concluded, from this figure that the general agreement between calculated and experimental values is qualitatively similar to that obtained for carbonyl compounds.

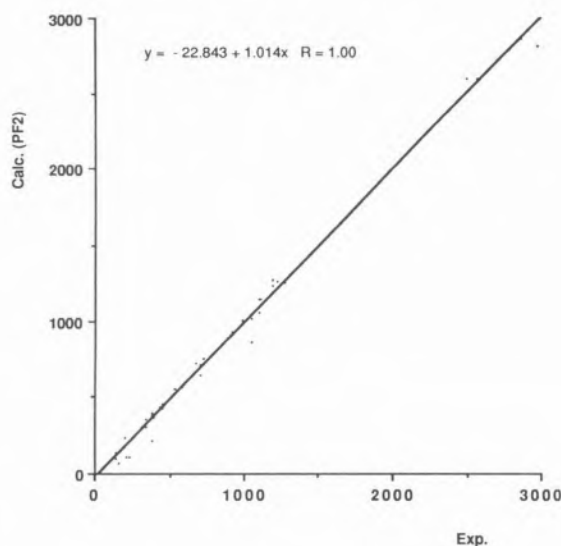


Figure 14 – Calculated (PF2) versus experimental vibrational frequencies ( $\text{cm}^{-1}$ ) for thiocarbonyl molecules. Data was taken from refs. 10, 12 and references therein.

## Acknowledgements

The author acknowledges both to Profs. J.J.C.Teixeira-Dias, Departamento de Química, Universidade de Aveiro (Portugal), and P.R.Carey, Case Western Reserve University, Cleveland, Ohio (USA), for their useful comments and suggestions on this paper and for their precious help during the PF1/PF2 force fields development. This work was financially supported by Junta Nacional de Investigação Científica e Tecnológica (J.N.I.C.T.), Lisboa (Portugal), Praxis XXI.

## References

1. T.L.Hill, *J.Chem.Phys.* **14** (1946) 465.
2. S.Lifson and A.Warshel, *J.Chem.Phys.* **49** (1968) 5116.
3. J.J.C.Teixeira-Dias and R.Fausto, *J.Mol.Struct.* **144** (1986) 199.
4. R.Fausto and J.J.C.Teixeira-Dias, *J.Mol.Struct.* **144** (1986) 215.
5. R.Fausto and J.J.C.Teixeira-Dias, *J.Mol.Struct.* **144** (1986) 225.
6. R.Fausto and J.J.C.Teixeira-Dias, *J.Mol.Struct.* **144** (1986) 241.
7. J.J.C.Teixeira-Dias and R.Fausto, *Pure and App.Chem.* **61** (1989) 959.
8. R.Fausto and J.J.C.Teixeira-Dias, *Proceedings of the 11<sup>th</sup> Meeting of the Portuguese Society of Chemistry*, Lisbon, Portugal, 1988, p.QF-CE5.
9. J.J.C.Teixeira-Dias and R.Fausto, *Rev.Port.Quím.* **29** (1987) 47.
10. R.Fausto, Ph.D.Thesis, The University Chemical Department, Coimbra, Portugal, 1987.
11. R.Fausto, J.J.C.Teixeira-Dias and P.R.Carey, *J.Mol.Struct.* **159** (1987) 137.
12. R.Fausto, J.J.C.Teixeira-Dias and P.R.Carey, *J.Mol.Struct.* **212** (1989) 61.
13. U.Burket and N.L.Allinger, "Molecular Mechanics", ACS Monograph 177, Am.Chem.Soc. Washington, USA, 1982.
14. S.R.Niketic' and K.Rasmussen, "The Consistent Force Field: A Documentation", Lecture Notes in Chemistry, Vol.3, Springer-Verlag, Heidelberg, FRG, 1977.
15. K.Rasmussen, "Potential Energy Functions in Conformational Analysis", Lecture Notes in Chemistry, Vol.37, Springer-Verlag, Heidelberg, FRG, 1985.
16. C.Altona and M.Sundaralingam, *J.Am.Chem.Soc.* **92** (1970) 1995.
17. E.M.Engler, J.D. Andose and P.V.R.Schleyer, *J.Am.Chem.Soc.* **95** (1973) 8005.
18. D.H.Wertz and N.L.Allinger, *Tetrahedron*, **30** (1974) 1571.
19. P.M.Morse, *Phys.Rev.* **34** (1929) 57.
20. A.Warshel, *J.Chem.Phys.* **55** (1971) 3327.
21. N.L.Allinger, M.T.Tribble, M.A.Miller and D.H.Wertz, *J.Am.Chem.Soc.* **93** (1971) 1637.
22. O.Ermer, *Tetrahedron*, **30** (1974) 3130.
23. H.Margenau and N.R.Kestner, "Theory of Intermolecular Forces", Pergamon Press, Oxford, U.K. 1969.
24. F.London, *Trans.Faraday Soc.* **33** (1937) 8.
25. K.S.Pitzer, *Adv.Chem.Phys.* **2** (1959) 59.
26. R.A.Buckingham, *Trans.Faraday Soc.* **54** (1958) 453.
27. J.E.Lennard-Jones, *Proc.Roy.Soc.* **43** (1931) 461.
28. N.L.Allinger, *J.Am.Chem.Soc.* **99** (1977) 8127.
29. N.L.Allinger and D.Y.Chung, *J.Am.Chem.Soc.* **98** (1976) 6798.
30. D.E.Williams, *J.Chem.Phys.* **43** (1965) 4424.
31. D.E.Williams and T.L.Starr, *Comput.Chem.* **1** (1977) 173.
32. U.Burket, *Tetrahedron*, **33** (1977) 2237.
33. T.Laier and E.Larsen, *Acta Chem.Scand.* **A33** (1979) 257.
34. G.Del Re, *J.Chem.Soc.* (1958) 4031.
35. S.Melberg and K.Rasmussen, *J.Mol.Struct.* **57** (1979) 215.
36. G.N.Ramachandram and K.Srinivasan, *Int.J.Protein Res.* **1** (1969) 5.
37. A.J.Hopfinger, "Conformational Properties of Macromolecules", Academic Press, New York, USA, 1973.
38. A.I.Kataigorodski, *Chem.Soc.Rev.* **7** (1978) 133.
39. G.J.Gleicher and P.V.R.Schleyer, *J.Am.Chem.Soc.* **89** (1967) 582.
40. K.B.Wiberg, *J.Am.Chem.Soc.* **87** (1965) 1070.
41. O.Ermer, "Aspekte von Kraftfeldrechnungen", Wolfgang Bauer Verlag, Munich, FRG, 1981.
42. A.Warshel and S.Lifson, *Chem.Phys.Lett.* **4** (1969) 255.
43. K.Kuchitsu and S.J.Cyvin, "Molecular Structures and Vibrations", Ed.S.J.Cyvin, Elsevier, Amsterdam, Neederlands, 1972, Cap.12.
44. K.Kuchitsu, "Critical Evaluation of Chem. and Phys. Structural Information", Ed.D.R.Lide and M.A.Paul, Nat.Acad.Sci. Washington, USA, 1974, p.132-139.
45. A.Cauchy, *Comp.Rend.Sci.(Paris)*, **25** (1847) 536.
46. P.E.Gill, W.Murray and S.M.Picker, *Natl.Phys.Lab.Report*, NAC 24, 1972.
47. W.C.Davidon, *AEC Res. and Develop.Report*, ANL-5990 (rev.), 1959.
48. R.Fletcher and M.J.Powell, *Comput.J.* **7** (1963) 149.
49. E.B.Wilson, *J.Chem.Phys.* **9** (1941) 76.
50. W.D.Gwinn, *J.Chem.Phys.* **55** (1971) 477.
51. R.Fausto, "Aplicações da Mecânica Molecular e da Espectroscopia Vibracional à Análise Conformacional", The University Chemical Department, Coimbra, Portugal, 1984.
52. K.Kimura and M.Kubo, *J.Chem.Phys.* **30** (1959) 151.
53. R.T.M.Lees and J.G.Baker, *J.Chem.Phys.* **30** (1968) 5299.
54. K.Tamagawa, M.Takemura, S.Konaka and M.Kimura, *J.Mol.Struct.* **125** (1984) 131.
55. M.Hayashi and K.Kuwada, *J.Mol.Struct.* **28** (1975) 147.
56. N.L.Allinger, M.T.Tribble and M.A.Miller, *Tetrahedron*, **28** (1972) 1173.
57. V.J.Klimkowski, P.V.Nuffel, L.V.D. Eenden, C.V.Alsenoy, H.J.Geise, J.N.Scarsdale and L.Schafer, *J.Comp.Chem.* **5** (1984) 122.
58. V.Sackwild and W.G.Richards, *J.Mol.Struct.* **89** (1982) 269.
59. R.Fausto, L.A.E.Batista de Carvalho, J.J.C.Teixeira-Dias and M.N.Ramos, *J.Chem. Soc. (Faraday Trans. II)*, **85** (1989) 1945.
60. M.Ohsaku, Y.Shiro and H.Murata, *Bull.Chem.Soc.Jpn.* **45** (1972) 954.
61. M.Ohsaku, Y.Shiro and H.Murata, *Bull.Chem.Soc.Jpn.* **46** (1973) 1399.
62. M.Hayashi, T.Shimanouchi and S.Mizushima, *J.Chem.Phys.* **26** (1957) 608.
63. N.Nogami, H.Sugeta and T.Miyazawa, *Bull.Chem.Soc.Jpn.* **48** (1975) 3573.
64. M.Sakakibara, H.Matsuura, I.Harada and T.Shimanouchi, *Bull.Chem.Soc.Jpn.* **50** (1977) 111.
65. J.R.Durig, D.A.C.Compton and M.R.Jalilian, *J. Phys.Chem.* **83** (1979) 511.
66. K.Oyanagi and K.Kuchitsu, *Bull.Chem.Soc.Jpn.* **51** (1978) 2243.
67. M.Adachi, J.Nakagawa and M.Hayashi, *J.Mol.Spectrosc.* **91** (1982) 381.
68. M.Hayashi, M.Adachi and J.Nakagawa, *J.Mol.Spectrosc.* **86** (1981) 129.
69. N.L.Allinger and M.J.Hickey, *J.Am.Chem.Soc.* **97** (1975) 5167.
70. M.Ohsaku and A.Imamura, *Mol.Phys.* **55** (1985) 331.
71. L.A.E.Batista de Carvalho, Ph.D.Thesis, The University Chemical Department, Coimbra, Portugal, 1989.
72. R.Fausto and J.J.C.Teixeira-Dias, *J.Mol.Struct.(Theochem.)*, **150** (1987) 381.
73. R.Fausto, J.J.C.Teixeira-Dias and P.R.Carey, *J.Mol.Struct.(Theochem.)*, **152** (1987) 119.
74. R.Fausto, J.J.C.Teixeira-Dias and P.R.Carey, *J.Mol.Struct.(Theochem.)*, **168** (1988) 179.